

# Automatic Sweat Pore Extraction Using Convolutional Neural Networks

Dennis Kovarik

Department of Computer Science and Engineering  
South Dakota School of Mines and Technology  
501 E. St. Joseph Street, Rapid City, USA, 57701  
dennis.kovarik@mines.sdsmt.edu

Mengyu Qiao

Department of Computer Science and Engineering  
South Dakota School of Mines and Technology  
501 E. St. Joseph Street, Rapid City, USA, 57701  
mengyu.qiao@sdsmt.edu

## **Abstract**

Fingerprint as one of the most widely used biometric characteristics presents distinctive patterns for person identification and authentication. Most automated Fingerprint Identification Systems use minutiae to match fingerprints. In comparison with patent fingerprints, latent fingerprints are more prevalent at crime scenes, but usually have poor quality. In this paper, we propose a method for extracting sweat pores from upconverting-nanoparticle enhanced fingerprint images by using convolutional neural networks. In this method, candidate sweat pores are identified by searching the local minimum pixel values along the ridgelines in the fingerprint. Then each candidate sweat pore is verified by using a convolutional neural network for classification. To create a stable and accurate model, we created a dataset of over ten thousand manually labeled samples containing valid and invalid sweat pores. In experiments, the proposed method achieved high accuracy in sweat pore extraction.

## I. Introduction

Fingerprint identification is the process of identifying individuals using their fingerprints [1]. Because of their uniqueness and permanence, fingerprints have been used to identify people since the 19<sup>th</sup> century [2]. A latent fingerprint is defined as “a fingerprint left on a surface by deposits of oils and/or perspiration from the finger” [3]. By collecting latent fingerprints found at crime scenes, law enforcement can use fingerprint identification in order to help link suspects to crimes [4]. There have been significant efforts in the past to automate this process, but despite the many advances made, it is still an area of continuing research.

A critical step in automatic fingerprint recognition systems is feature extraction. In this step, computational methods are used to identify and extract characteristic, quantifiable, and comparable features from the fingerprint. These features can be placed into 3 categories, which are referred to as level 1, level 2, and level 3 features. Level 1 features are the general patterns exhibited by the ridge orientations. Examples of these patterns include whorls, loops, and arches. Level 2 features refer to certain points found on the fingerprint, which are called minutiae. These minutiae usually identify the ridge endings and ridge bifurcations (where the ridge splits into two) that are found on the fingerprint. Finally, level 3 features include features such as sweat pore configurations and the ridge contours [5].

The features extracted during the feature extraction step are used in the matching step. During this step, the extracted features are used in a matching algorithm to determine how similar the captured fingerprint is to another fingerprint stored in some databases [6]. Most automatic fingerprint recognition systems extract and use level 2 features to match the fingerprints, but the poor quality of most latent fingerprints makes it difficult to extract sufficient high-quality features to support accurate matching. Therefore, researchers are looking into incorporating level 3 features in order to improve the accuracy in the matching different fingerprints [7]. Since sweat pores are grouped more tightly together, using sweat pores would allow for more features to be extracted from a smaller area of the fingerprint.

Multiple attempts have been made to extract sweat pores from fingerprints. For example, Ray et al. proposed a pore extraction method through the implementation of a modified minimum squared error approach [8]. Zhao et al. proposed an adaptive modeling technique in which they extracted sweat pores by using adaptively generated pore models [9]. Jang et al. used deep neural networks to identify pores, after which they would “refine the pore information by finding local maxima to identify pores with different intensities in the fingerprint image” [10]. Genovese et al. proposed a technique to extract sweat pores from touchless fingerprint images. Their technique involved extracting candidate pores by using a gamma transform to analyze the image at different contrast conditions [11].

The purpose of this study is to develop a method to automatically extract sweat pores from images of latent fingerprints collected by using upconverting nanoparticles exhibiting near infrared NIR-to-NIR upconversion luminescence. The extracted sweat pores could then be used to help match the fingerprints. This study is a part of a larger project which is

developing a portable field system to collect sensitive, interference-free latent fingerprints using these upconverting nanoparticles. The latent fingerprints collected using these nanoparticles results in images that look much like that presented in Figure 1. This study aims to develop part of the software, for this device, that will perform the automatic fingerprint recognition.



Figure 1: Original Latent Fingerprint

## II. Proposed Approach

### 2.1. Image Pre-processing

To facilitate sweat pores extraction, several images produced from the fingerprint filtering and enhancement were used. All images in the following description were of the same size and corresponded to the same fingerprint. Furthermore, a certain location in one image corresponded to the same location in all the other images. The first of which was a grayscale version of the original image. This image will be referred to as the “Grayscale Fingerprint Image”. By converting the image to grayscale, we reduce the complexity of the features to be extracted. In color images, each pixel is represented by 3 separate values for the colors red, green, and blue, while pixels in grayscale images are only represented by one value (ranging from 0 to 255 for 8-bit grayscale). Because of this, it is simpler to extract features from grayscale images than from color images. The second type of image utilized was the binary version of the filtered and enhanced grayscale image. This image will be referred to as the “Binary Enhanced Image”, and it can be seen in Figure 2. In this image, the values for each pixel can only be 0 or 1, where 1 indicates that the pixel is part of a ridge while 0 indicates that it is not. In this way, the image clearly defines where all the ridges exist in the fingerprint image [12]. The third image used was a version of the binary enhanced image in which each of the ridges were thinned down to be a single pixel wide. This image will be referred to as the “Thinned Binary Enhanced Image”. This image would be used to define the locations of the ridgelines in the “Grayscale Fingerprint Image”.



Figure 2: Binary Enhanced Fingerprint Image

## 2.2. Sweat Pore Extraction

The algorithm to extract the sweat pores from the images of latent fingerprints had 3 main steps as shown in Figure 3. In the first two steps, candidate pores would be identified by finding the local minima along the ridges and by performing adaptive thresholding to these identified local minima. Finally, each of the candidate sweat pores would be classified as sweat pore or not by using a convolutional neural network.

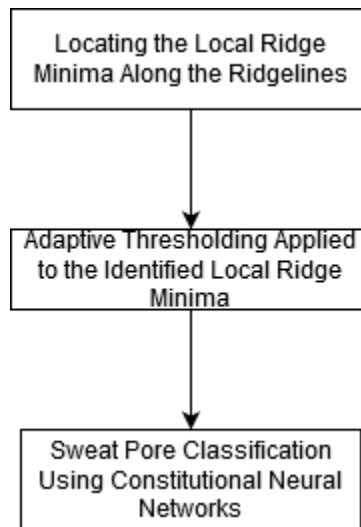


Figure 3: Sweat Pore Extraction Steps

### 2.2.1. Locating Local Minima Along Ridgelines

Candidate sweat pores in the latent fingerprint were identified by following the ridgelines and marking the minimum pixel values that were both within a certain distance from a reference pixel location and on a previously identified ridge. The candidate sweat pores were extracted from the "Grayscale Fingerprint Image". The "Thinned Binary Enhanced Image" was used to identify the ridgelines for the latent fingerprint in the "Grayscale Fingerprint Image", while the "Binary Enhanced Image" was used to define the locations of the ridges in the image. For each white pixel along the ridgelines identified in the

“Thinned Binary Enhanced Image”, the minimum pixel value in the “Grayscale Fingerprint Image”, that was both on a ridge (defined by the “Binary Enhanced Image”) and within 6 pixels from the location of the reference pixel, was marked and stored in a separate temporary image (that was of the same size all the other images) referred to as the “Ridge Minima Image”. The identified minimum values (stored in the “Ridge Minima Image”) were stored in the same locations (the same row and column) as each of the reference pixels found in the “Thinned Binary Enhanced Image”. This operation would result in the “Ridge Minima Image” looking much like the “Thinned Binary Enhanced Image”, except that each pixel along the ridgelines found in the “Ridge Minima Image” would hold the minimum pixel value found in the “Grayscale Fingerprint Image” that is both on a ridge and within 6 pixels from the same location as the reference pixel.

The plotted “Ridge Minima Image” looks like a sinusoidal wave, where the pixel values would alternate between going up and down in value as you move along the ridge. The idea for this algorithm is that the locations of the local minimums present along this wave would represent locations along the ridgelines where the sweat pores are most likely to exist at. So, the local minimums along the ridgelines in the “Ridge Minima Image” were marked. From this, the original pixel locations of the minimum pixel values along the ridges present in the “Grayscale Fingerprint Image” were identified and marked. By doing this, the majority of the sweat pores in the latent fingerprint were identified, but many false sweat pores were also created in the process. To eliminate these false pores, adaptive thresholding was then performed on the marked candidate pores.

### **2.2.2. Adaptive Thresholding**

The adaptive thresholding operation again involved using the “Binary Enhanced Image” to determine which pixels in the “Grayscale Fingerprint Image” were located on a previously identified ridge. For each of the marked candidate sweat pores, the local average pixel value within 5 pixels from that same location in the “Grayscale Fingerprint Image” was calculated. After this, adaptive thresholding was performed by comparing the calculated local average pixel value with the pixel value for the candidate sweat pore. If the pixel value for the candidate sweat pore was greater than the local average, then the candidate sweat pore would be unmarked and disregarded. Those candidates with a pixel value less than or equal to the local average were left marked and were further considered to be candidate sweat pores. As a result of these steps, an image that looks much like that found in Figure 4 was produced, where each green dot represents a candidate sweat pore found within the “Grayscale Fingerprint Image”. Even though the adaptive thresholding helped to remove some of the false sweat pores, the number of false sweat pores remaining was still unacceptable. In order to further reduce the number of false sweat pores, a convolutional neural network was used to classified each of the candidate sweat pores as a sweat pore or not.

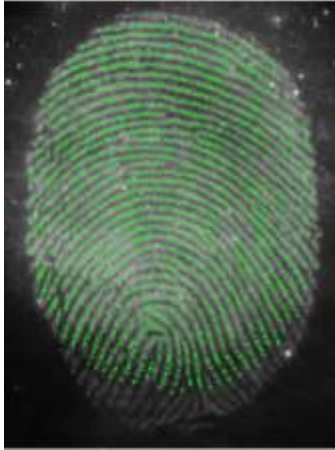


Figure 4: Candidate Sweat Pores

### 2.2.3. Sweat Pore Verification Using Convolutional Neural Networks

A convolutional neural network was built to verify the candidate sweat pores. The neural network input layer accepted images that were 25 by 25 pixels in size. The neural network had 3 inner convolutional layers. The first and last inner layer had 32 filters each with a size of 3-by-3, while the middle convolutional layer had 32 filters each with a size of 4-by-4.

A dataset of over 2800 unique images was compiled for training the neural network. In this dataset, there were over 1300 images classified as not a sweat pore while over 1500 were classified as a sweat pore. These images were collected from 3 other grayscale images of latent fingerprints, and each of the collected images of a candidate sweat pore used in training the neural network was a 25-by-25-pixel image. Each of these images were manually classified as a sweat pore or not a sweat pore. Furthermore, for each unique image collected, around ten more images were generated, where each of the newly generated images was a brightened or dimmed version of the original image. In all, the final dataset used to train the neural network consisted of over 25000 grayscale images, where each image was 25-by-25 pixels in size.

Training the neural network was completed using the stochastic gradient descent with momentum optimizer with a constant learning rate of 0.001. The neural network was allowed to train for 11 minutes and 30 seconds, which allowed for 11 epochs to elapse. The final training validation accuracy was 98.09%.

Additionally, after the sweat pores were classified, clusters of sweat pores (where the sweat pores were within 3 to 5 pixels of each other) were replaced with the one pore in the cluster that had the highest probability of being a sweat pore.

### III. Results and Discussion

The images used in the dataset to train the neural network were obtained from 3 images of latent fingerprints, while validation of the algorithm was completed using a 4<sup>th</sup> image of a latent fingerprint. This 4<sup>th</sup> image will be referred to as the validation image. The results were determined by comparing the automatically extracted sweat pores against sweat pores that were extracted manually.

In total, the algorithm correctly extracted 533 sweat pores from a total of 637 manually extracted sweat pores. Additionally, 97 false sweat pores were created by the above algorithm. A visual representation of this can be seen in Figure 5, where the green dots are the correctly extracted sweat pores, red dots are false sweat pores, and the blue dots are the manually extracted sweat pores that the algorithm failed to identify. These results are also summarized in table 1. Around 83% of the manually identified sweat pores were successfully extracted automatically, while only 15% of all automatically extracted sweat pores were false sweat pores.



Figure 5: Extraction Results Comparison Image (Green: True Positives, Red: False Positives. Blue: False Negatives)

	Number of Pores	Percent of all Manually Extracted Pores	Percent of all Automatically Extracted Pores
True Positives	533	83.67%	84.60%
False Positives	97	NA	15.40%
False Negatives	104	15.61%	16.51%
Total Pores Extracted Manually	637	100%	NA
Total Pores Extracted Automatically	630	NA	100%

Table 1: Summary of Results



These results are promising for the small dataset of latent fingerprints used to train the neural network. Better results could be obtained if a larger dataset from more images of latent fingerprints were made available. In addition, more accurate results could be obtained if the current dataset was verified and refined by experts.

## **IV. Conclusion**

### **4.1. Summary**

Most of the valid sweat pores were identified by marking the local minimum pixel values along the ridgelines. By performing adaptive thresholding on the candidate sweat pores, the number of false sweat pores was able to be reduced. Furthermore, classifying the remaining candidate sweat pores using a convolutional neural network further reduced the number of false pores. Of all the sweat pores that were manually extracted, around 83% of them were successfully extracted automatically by the proposed approach. In addition, of all sweat pores extracted automatically, only 15% of them were false sweat pores.

Since data used to train the neural network was collected from a small set of images of latent fingerprints, better results are expected by expanding the current dataset. In addition, validation of the images in the current dataset could lead to further enhancement of the feature extraction.

### **4.2. Future Work**

The current data set used to train the neural network will need to be verified and expanded on in order to provide better results. Work will need to be done on extracting other level 3 features from the latent fingerprints. By mitigating unfavorable factors in the use of latent fingerprint, a comprehensive scheme based on the fusion of diverse features of Level 1-3 is expected to achieve high accuracy and reliability. In addition, the extracted features will need to be represented in a way that would facilitate the ability to match fingerprints against a large database of fingerprints. One possible avenue to accomplish this is to investigate using machine learning for matching fingerprints.

## **Acknowledgment**

This work was supported by the National Science Foundation through the REU Site: Security Printing and Anti-Counterfeiting Technology (SPACT) under NSF award numbers (EEC-1852336). This work was partially supported by the National Institute of Justice grant 2017-IJ-CX-0026. Opinions, findings, and conclusions or recommendations expressed in this publication are those of the authors and do not necessarily reflect the views of the Department of Justice. I would like to thank Dr. Mengyu Qiao for advising me on this project. Special thanks to Dr. William Cross, Dr. Jon Kellar, and Dr. Grant Crawford for their continuous support, feedback, and guidance on this project. In addition, I would like to acknowledge Dr. Rodney Rice for his help in developing the framework

and sharing his expertise in technical writing. Lastly, thanks to Dr. Grant Crawford and the SPACT Committee for selecting me to participate in this summer REU.

## References

- [1] Mayhew, S., What is Fingerprint Identification? Retrieved August 2, 2019, from <https://www.biometricupdate.com/201205/what-is-fingerprint-identification>
- [2] Watson, S., How Fingerprinting Works. Retrieved June 19, 2019, from <https://science.howstuffworks.com/fingerprinting3.htm>
- [3] US Legal, Inc. (n.d.). Latent Fingerprint Law and Legal Definition. Retrieved July 29, 2019, from <https://definitions.uslegal.com/l/latent-fingerprint/>
- [4] Fingerprints: An Overview. (2016, June 8). Retrieved June 19, 2019, from <https://nij.gov/topics/forensics/evidence/impression/Pages/fingerprints.aspx>
- [5] Bansal, R., Sehgal, P., & Bedi, P. (2011). Minutiae Extraction from Fingerprint Images-a Review. *International Journal of Computer Science Issues (IJCSI)*, 8(5), 74.
- [6] Ratha, N. K., & Bolle, R. (2011). *Automatic fingerprint recognition systems*. New York: Springer.
- [7] Nguyen, D. and Jain, A. (2019). End-to-End Pore Extraction and Matching in Latent Fingerprints: Going Beyond Minutiae. GroundAi. [online] Available at: <https://www.groundai.com/project/end-to-end-pore-extraction-and-matching-in-latent-fingerprints-going-beyond-minutiae/1#bib.bib2> [Accessed 19 Jul. 2019].
- [8] Ray, M., Meenen, P., & Adhanii, R. (n.d.). A novel approach to fingerprint pore extraction. *Proceedings of the Thirty-Seventh Southeastern Symposium on System Theory, 2005. SSST 05*. doi:10.1109/ssst.2005.1460922
- [9] Zhao, Q., Zhang, D., Zhang, L., & Luo, N. (2010). Adaptive fingerprint pore modeling and extraction. *Pattern Recognition*, 43(8), 2833-2844. doi:10.1016/j.patcog.2010.02.016
- [10] Jang, H., Kim, D., Mun, S., Choi, S., & Lee, H. (2017). DeepPore: Fingerprint Pore Extraction Using Deep Convolutional Neural Networks [Abstract]. *IEEE Signal Processing Letters*, 24(12), 1808-1812. doi:10.1109/lsp.2017.2761454
- [11] Genovese, A., Munoz, E., Piuri, V., Scotti, F., & Sforza, G. (2016). Towards touchless pore fingerprint biometrics: A neural approach. *2016 IEEE Congress on Evolutionary Computation (CEC)*. doi:10.1109/cec.2016.7744332
- [12] Cao, K., & Jain, A. K. (2018, March 22). Automated Latent Fingerprint Recognition (Rep. No. 18502999). doi:10.1109/TPAMI.2018.2818162
- [12] Kovesi, P. (2005). Retrieved from <https://www.peterkovesi.com/matlabfns/#fingerprints>